Simulation of an ensemble of $N_f = 2 + 1 + 1$ twisted mass clover-improved fermions at physical quark masses

Jacob Finkenrath[1,⋆], *Constantia* Alexandrou[1,2], *Simone* Bacchio[2,3], *Panagiotis* Charalambous[1,2], *Petros* Dimopoulos[4,5], *Roberto* Frezzotti[4], *Karl* Jansen[5], *Bartosz* Kostrzewa[6], *Giancarlo* Rossi[4,5], and *Carsten* Urbach[6]

[1]*Computation-based Science and Technology Research Center, The Cyprus Institute, Nicosia, 20, Constantinou Kavafi Str., Nicosia 2121, Cyprus*

[2]*Department of Physics, University of Cyprus, P.O. Box 20537, Nicosia 1678, Cyprus*

[3]*Bergische Universität Wuppertal, Wuppertal, Germany*

[4]*Dipartimento di Fisica, Università di Roma "Tor Vergata" and INFN, Sezione di Roma 2, Via della Ricerca Scientifica - 00133 Rome, Italy*

[5]*Centro Fermi - Museo Storico della Fisica e Centro Studi e Ricerche Enrico Fermi, Compendio del Viminale, Piazza del Viminiale 1, I-00184, Rome, Italy*

[6]*NIC, DESY, Zeuthen, Germany*

[7]*HISKP (Theory), Rheinische Friedrich-Wilhelms-Universität Bonn, Bonn, Germany*

Abstract. We present a general strategy aimed at generating $N_f = 2 + 1 + 1$ configurations with quarks at their physical mass using maximally twisted mass fermions to ensure automatic $O(a)$ improvement, in the presence of a clover term tuned to reduce the charged to neutral pion mass difference. The target system, for the moment, is a lattice of size $64^3 \times 128$ with a lattice spacing $a \sim 0.08$ fm. We show preliminary results on the pion and kaon mass and decay constants.

1 Introduction

During the last decade, lattice QCD simulations with light quarks having physical masses on large enough volumes have become feasible owing to improvements in lattice actions and numerical algorithms as well as due to steadily increasing computational power. In this work, we illustrate a strategy aimed at generating $N_f = 2 + 1 + 1$ configurations with quarks at the physical mass using maximally twisted fermions to ensure automatic $O(a)$ improvement. This bonus does not come without a price, as the twisted regularization breaks isospin leading to an undesired (negative) neutral pion to charged mass splitting. It has been shown in [1] that a suitably tuned clover term can ease the problem and allow for stable simulations at affordable lattice spacings and volumes (sec. 2). The tuning procedure is quite complicated as a number of parameters (bare quark masses, critical mass, and the clover term coefficient, c_{SW}) have to be simultaneously set at appropriate values. In sec. 3 we discuss a viable strategy that allows with relative small effort and good signal-to-noise ratio to desired tuning in a way that weakly depends on the light quark sector. Going to large lattice volumes, as needed to simulate

---

⋆Speaker, e-mail: j.finkenrath@cyi.ac.cy

pions with close-to-physical mass, leads to an increased density of very small Dirac operator eigenvalues, which is expected to stabilise the MD behaviour of HMC-like algorithms but also requires the use of very well preconditioned and efficient linear solvers. We will discuss the practical aspects of our Monte Carlo simulation strategy and related issues in sec. 4. Finally in sec. 5, we will present results on the pion and kaon masses and decay constants using the $N_f = 2 + 1 + 1$ ensemble.

2 Setup

The action used in our simulation is given by

$$S = \beta \cdot S_g - \chi_\ell^\dagger \{D^\dagger(\mu_\ell)D(\mu_\ell)\}^{-1}\chi_\ell - \chi_h^\dagger \{D_{1+1}^\dagger(\mu_\sigma, \mu_\delta)D_{1+1}(\mu_\sigma, \mu_\delta)\}^{-1/2}\chi_h \tag{1}$$

with S_g the Iwasaki improved gauge action [2], β the bare coupling constant and χ_ℓ and χ_h pseudofermion fields. The light quark-doublet is made of the up- and down-quarks, described in the isospin symmetric limit by a degenerated twisted mass operator with twisted mass parameter μ_ℓ. The heavy quark doublet is made by the strange and charm quarks and are described by the mass non-degenerated twisted mass operator given by

$$D_{1+1}(\mu_\sigma, \mu_\delta) = D_W(\kappa, c_{sw}) \otimes 1 + i\mu_\sigma(\gamma_5 \otimes \tau_3) - \mu_\delta(1 \otimes \tau_1) = \begin{bmatrix} D_W + i\gamma_5\mu_\sigma & -\mu_\delta \\ -\mu_\delta & D_W - i\gamma_5\mu_\sigma \end{bmatrix} \tag{2}$$

with bare mass parameter μ_σ and μ_δ. The Wilson Dirac operator $D_W(\kappa, c_{sw})$ depends on the bare mass parameter $\kappa = \frac{1}{2(4+m)}$. A Sheikholeslami–Wohlert-term [3] is added. For degenerated masses one gets that $\det\{D^\dagger(\mu_\ell)D(\mu_\ell)\} = \det\{D_{1+1}(\mu_\ell, 0)\}$.

In the twisted mass discretization of lattice QCD all the correlators that are expectation values of parity even multilocal operator products are by symmetry free of linear lattice artefacts if the Partially Conserved Axial Current (PCAC) mass vanishes, which is equivalent to tuning the bare mass parameter $\kappa(m)$ to its critical value [4, 5]. In this case, the renormalized light quark mass is at maximal twist and related to $m_\ell = \mu_\ell/Z_P$ with Z_P the pseudoscalar renormalization constant. This fine tuning of $\kappa(m) \to \kappa_{crit}(m)$ will be discussed in the next section.

The twisted mass Wilson-Dirac operator corresponding to the light quark sector is protected from zero eigenmodes for a finite twisted mass term $\mu_\ell > 0$. In fact $D^\dagger(\mu_\ell)D(\mu_\ell) = D_W^\dagger D_W + \mu_\ell^2$ with $\min\{\lambda\} \geq \mu_\ell$. From a numerical point of view this holds the promise to be able to reach small quark masses with $\mu_\ell > 0$ including the physical value.

However, the lattice regularization breaks some continuum symmetries that are recovered after extrapolating to zero lattice spacing. Besides the breaking of the chiral symmetry due to the Wilson term, a finite twisted mass term breaks isospin symmetry by introducing a mass-splitting in the pion triplet.

The neutral to charge pion mass splitting can be estimated in chiral perturbation theory. To first order one finds [6]

$$(m_{\pi^0}^2 - m_{\pi^\pm}^2) \approx 4 \cdot c_2 \cdot a^2 \tag{3}$$

where c_2 depends on low energy constants and it is found to be negative for twisted mass fermions [7]. This means that the neutral pion mass may vanish for finite light quark masses triggering a phase transition into a non-physical phase induces by lattice artefacts.

In Fig. 1 we show the isospin mass splitting between the charged and neutral pion. For $N_f = 2 + 1 + 1$ twisted mass fermion ensembles with $c_{SW} = 0$ the mass splitting between the neutral and charged pions is sizable for the three different lattice spacings examined. It follows that for lattice spacing $a \gtrsim 0.05$ fm the neutral pion mass would vanish for physical light quark masses making

simulation at the physical point impossible. However, it was shown that by adding a clover term the isospin breaking effects can be suppressed [1]. This was demonstrated in the case of the $N_f = 2$ twisted mass fermion ensembles with $c_{SW} = 1.57551$ and a lattice spacing of $a = 0.0938$ fm. In particular, for a charged pion mass of $m_\pi = 130$ MeV the pion mass difference between the neutral and charge pions is smaller than $\sqrt{|m_{\pi^0}^2 - m_{\pi^\pm}^2|} \lesssim 6$ MeV and simulation of twisted mass fermions at physical light quarks are possible for $a < 0.1$ fm.
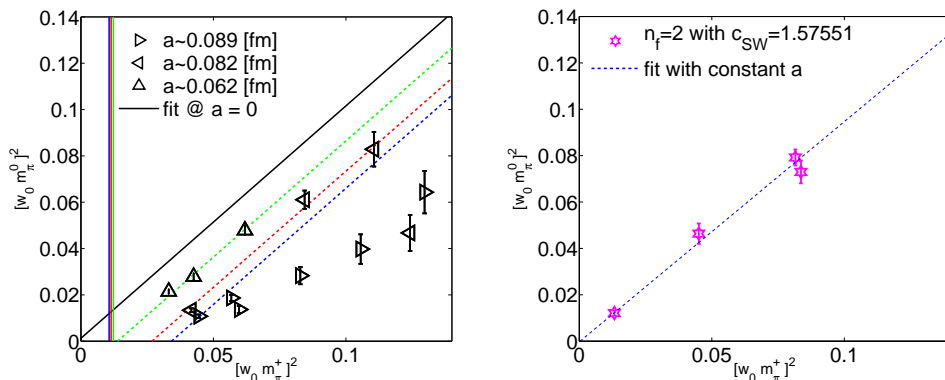
Figure 1. Left: The squared neutral pion mass is plotted against the squared charged pion mass in units of w_0 for $N_f = 2 + 1 + 1$ ETMC ensembles with no clover term i.e. taking $c_{SW} = 0$. We use a generalized fit excluding ensembles with $m_\pi > 400$ MeV and show results for three lattice spacings and extrapolating to $a = 0$. The line corresponds to the physical value of the charged pion mass. We used the definition of [8] for w_0. Right: The neutral pion mass for the $N_f = 2$ ensemble with a clover term.

3 Tuning towards physical quark masses

We start by discussing the tuning procedure towards physical quark mass, using the $N_f = 2 + 1 + 1$ twisted mass fermion discretization at a target lattice spacing of $a \sim 0.8$ fm. The inclusion in the action of a clover term suppresses isospin violation effects. Using an estimate from 1–loop tadpole boosted perturbation theory given by $c_{SW} \cong 1 + 0.113 g_{plaq}^2$ [9] with $g_{plaq}^2 = g_0^2/P$ and P the plaquette expectation value. This yields $c_{SW} = 1.69$. The tuning procedure consists of two major parts: i) tuning towards the critical mass and ii) tuning the heavy quarks towards their physical values. The two steps are strongly correlated. To tune to critical mass we use the vanishing of the PCAC mass, which depends on the light valence quarks and to tune the strange and charm quark masses we use dimensionless rations depending only on the strange and charm valence quarks.

V	β	μ_ℓ	μ_σ	μ_δ	κ	c_{SW}
128×64^3	1.778	0.00072	0.1246864	0.1315052	0.1394265	1.69

Table 1. The table shows the parameter used in the simulations of the target ensemble with pion masses close to the physical point.

For the tuning towards the critical mass we impose [10]

$$\frac{Z_A m_{PCAC}(\kappa)}{\mu_\ell} \lesssim 0.1 \qquad (4)$$

with Z_A the axial renormalization constant roughly given by ~ 0.8. For the tuning of the heavy quark masses, we introduce an additional step by setting the mass parameters μ_s and μ_c of the Osterwalder Seiler fermions such that

$$A_1 = \frac{\mu_c}{\mu_s} \equiv 11.8 \qquad \text{and} \qquad B_2 = \frac{m_{D_s}}{f_{D_s}} \equiv 7.9 . \qquad (5)$$

The final step is to match the masses of the Kaons involving an Osterwalder Seiler and a non-degenerated twisted mass valence strange quark, respectively. In this way the matching of valence and sea quark mass parameters is independent of finite size effects and with a negligibly small dependence on the light quark mass entering only through sea quark effects.

The approach was as follows

- We start with simulation using lattices of spatial extent $N_s = 24$ at four different mass values κ and $m_\pi \sim 310$ MeV. The parameters β and μ_σ, μ_δ are initially estimated by a set of preliminary studies aimed at investigating their interdependencies [11]. Using a linear fit for the PCAC mass as a function of the bare light quark mass parameter we estimate κ_{crit} as shown in Fig. 2) and recheck the value of c_{sw} and the lattice spacing a by using Wilson flow observables.

- With the estimated critical mass value we simulate a larger lattice size with spatial extent $N_s = 32$ and we check and re-tune the heavy quark masses by calculating the properties of the kaon and D-mesons.

- Based on the re-tuned heavy quark parameters μ_σ and μ_δ we run three simulations again with spatial lattice size $N_s = 32$ at different κ values and a pion mass of $m_\pi \sim 230$ MeV. Again we estimate the critical mass by using a linear fit to the PCAC mass for the generated ensembles as shown in Fig. 2. We then cross-check the estimated value by simulating an ensemble with a pion mass $m_\pi \sim 180$MeV.

- Finally we simulate our target lattice size with $N_s = 64^3$ and temporal extent $N_T = 128$ using pion masses close to the physical value.
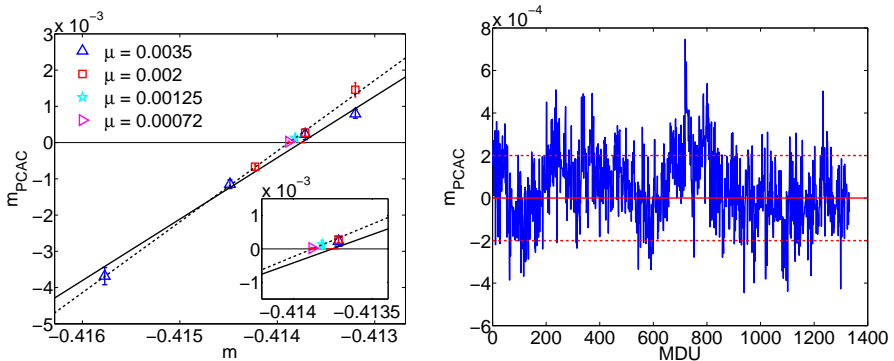

Figure 2. Left: PCAC mass versus κ in the tuning. Blue triangles are for the lattices $N_s = 24$, the red symbols for the lattices $N_s = 32$, the cyan star for a lattice of $N_s = 32$ with a pion mass of $m_\pi \sim 180$ MeV and the magenta point corresponds to the target ensemble with $N_s = 64$. Right: The history of the PCAC mass of our target lattice in units of molecular dynamics (MDU).

The PCAC masses of the target ensemble are shown Fig. 2 and final tuned parameters are found in Table 1. On the first 1200 MDUs we find that the average PCAC mass satisfies $|m_{PCAC}| < 0.00005$, which fulfills the bound given in Eq. (4) that ensures sufficient suppression of the linear lattice artefacts.

4 Stable algorithms

We use the Hybrid Monte Carlo (HMC) algorithms [12] with Hasenbusch mass-preconditioning [13] for the light quark sector and the rational HMC [14] for the heavy quark sector. The software package *tmLQCD* [15] with the multi-grid solver DDalphaAMG [16] is employed. For the inversions of the light and heavy quark sector a three-level DD-αAMG solver [17, 18], and even-odd preconditioned conjugate gradient (CG) solver and a multi-mass shifted CG solver are used (see Ref. [19] for more details). The gauge fields are integrated by using a 6-level nested minimal norm scheme of second order. We show the distribution of the maximal force terms for the light and heavy quark sectors in Fig. 3. The rational approximation is done for the interval [0.000014 1] by involving 10 terms, while a correction term is included in the acceptance step. Using 12 integration steps on the outer level and 384 on the inner level, the integration with length $\tau = 1$ yields a stable simulation, where the maximal energy violation is given by $\max(\delta H) = 5.67$ with an acceptance ratio of 77%.
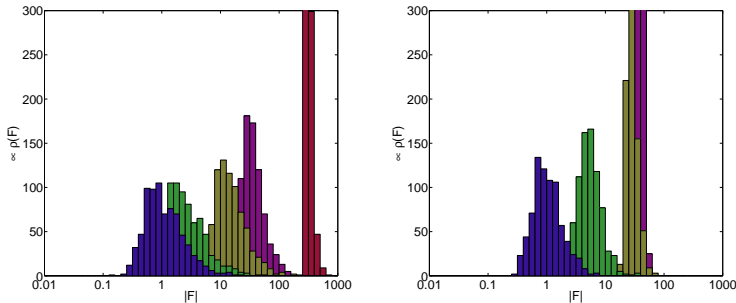

Figure 3. Left: Distribution of the maximal norm in the force terms of the light quark sector, where the force terms depending on the largest Hasenbusch mass-shift are shown in blue for $\rho = 0.003$, in green for $\rho = 0.0012$, in yellow for $\rho = 0.01$ and in purple for $\rho = 0.1$. The force term for the full operator is shown in red. Right: The Distribution of the maximal norm of the force terms, which are involved in the rational approximation. The distribution in blue corresponds to the terms $i = 9, 10$, in green to the terms $i = 7, 8$, in yellow to the terms $i = 6, 5, 4$ and in purple to the terms $i = 3, 2, 1$ in the rational approximation. The smallest shift is given by $i = 10$.

In the case of the plaquette it can be seen that the use of the Hasenbusch mass-preconditioning yields a quite stable run. As shown in Fig. 4 the history of the plaquette shows some larger oscillations for MDU< 800. This provides an estimate for the integrated autocorrelation time τ_{int}. We find $\tau_{int} = 31(13)$. Similar oscillations are found in the history of the PCAC mass, also shown in Fig. 2. They are seen to be anticorrelated with the plaquette oscillations. Nevertheless, we find that other observables, such as the topological charge, are not affected, and shows frequent oszillations. As shown in Fig. 4 the algorithm can efficiently sample the topological charge with an autocorrelation time of $\tau_{int} = 8(3)$.

5 Observables

In this section, we show preliminary results extracted from two-point functions using our target ensemble of tab. 1. See Ref.[20] for a detailed discussion on how these measurements are performed. In the left panel of Fig. 5 we show the pion mass dependence of the pion decay constant f_π in comparison with results obtained using $N_f = 2 + 1 + 1$ twisted mass fermions with $c_{SW} = 0$ and smallest pion
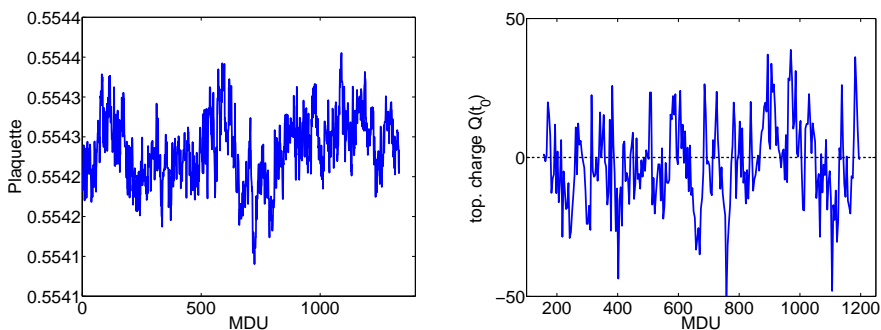
Figure 4. Left: The history of the plaquette. Right: The history of the topological charge defined using the gauge expression at gradient flow time $t = t_0$, is shown.
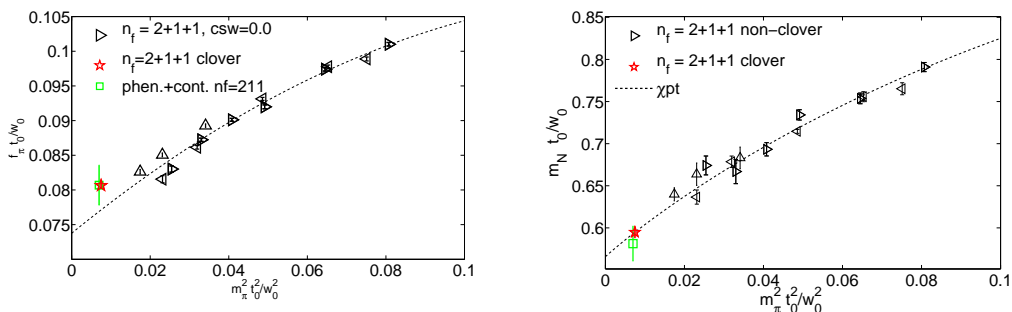

Figure 5. Left: The pion decay constant f_π is plotted against the pion mass in units of $t_0/w_0 a$. We show results for $N_f = 2 + 1 + 1$ ensembles without a clover term for three different values of β (triangles, black), The red star shows the pion decay constant of our target ensemble with $c_{SW} = 1.69$. The continuum value is shown by the green square. Right: We give results on the nucleon mass m_N from our target ensemble (red star) compared with results obtained using $N_f = 2 + 1 + 1$ twisted mass ensembles without a clover term (open triangles). DIfferent triangle orientations correspond to different lattice spacings with $a \sim 0.89$ fm for the orientation "to the right", $a \sim 0.82$ fm for "to the left" and $a \sim 0.67$ fm for "up".

mass of around $m_\pi \sim 210$ MeV in units of the gradient flow observables $t_0^2/w_0^2 a^2$. The results are fitted to a quadratic function in m_π^2 to guide the eye. Note that finite size effects were not corrected. The measured pion decay constant of our target ensemble agrees with the continuum value, which was determined using continuum extrapolations of the gradient flow observables determined in[8] and a pion decay constant of 130.2 MeV.

In the right panel of Fig. 5 we show the nucleon mass m_N in units of $t_0^2/w_0^2 a^2$ as a function of the charged pion mass squared m_π^2. We fit the results using $N_f = 2 + 1 + 1$ twisted mass fermion ensembles without a clover term with the help of leading order chiral perturbation theory [21, 22]. The agreement between the chirally extrapolated value with the value obtained using our current physical $N_f = 2 + 1 + 1$ ensemble indicates small cut-off effects for the nucleon mass in agreement with previous observations [23].

In the heavy quark sector, we use our tuned values of the strange and charm quarks to evaluate the decay constant of the kaon and D-mesons. In Fig. 6 we show the ratio of the pseudoscalar mass over the pseudoscalar decay constant as a function of the pion mass and compare it to the value obtained using the physical $N_f = 2$ ensemble with a clover term [1]. The ratio involving the D-meson agrees with the expectation while the ratio by the Kaon is above the physical value. A possible reason for this behavior could be the tuning conditions which primarily affects the charm quark mass possibly yielding large cut-off effects.
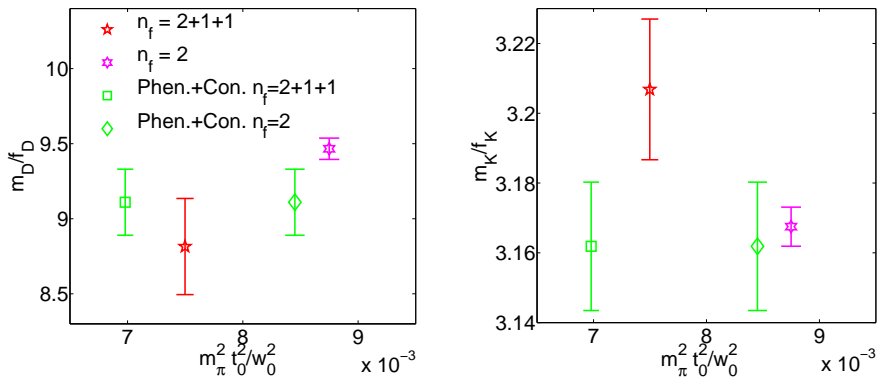
Figure 6. Left: The ratio of the decay constant of the D-meson over its mass for the $N_f = 2 + 1 + 1$ ensemble (red star) and for the $N_f = 2$ twisted mass clover ensemble with a pion mass of $m_\pi = 130$ MeV (magenta star). The green symbols correspond to the continuum points, using continuum extrapolated gradient flow observables t_0 and w_0 for $n_f = 2 + 1$ in [8] (square) and for the $N_f = 2$ in [24] (diamond). Right: The ratio of the decay constant of the kaon over its mass as a function of the pion mass in units of t_0^2/w_0^2 with the same symbols as those used for the D-meson.

6 Conclusion

In this work we illustrate how it is possible to set up stable simulations for $N_f = 2 + 1 + 1$ twisted mass fermions with a clover term to maximal twist and approximately physical values of the light, strange and charm quark masses. Introducing a clover term help to supress isospin breaking effects in the pion triplet and makes the simulation within the twisted mass fermion approach at the physical point feasible. Our tuning conditions for fixing the heavy quark masses and the light bare quark mass to maximal twisted are presented. Moreover, we show that, by using Hasenbusch–mass preconditioning combined with the RHMC, simulations are stable and that the force terms are under control. Using the $N_f = 2 + 1 + 1$ ensemble we show results on the pion decay constant, the nucleon mass and the ratios of the pseudoscalar mass over the decay constant [20]. We find a nucleon to pion mass ratio $m_N/m_\pi = 6.87(7)$ and kaon and D-meson mass ratio $m_K/m_\pi = 3.58(2)$ and $m_D/m_\pi = 13.2(9)$. Additional we listed pseudoscalar meson masses and their ratio with their decay constant in tab. 2. The lattice spacing as determined from the nucleon mass turns out to be $a \sim 0.082(2)$ fm.

Table 2. In the table are listed the masses and the decay constants of the charged pseudoscalar mesons.

am_π	0.0567(2)	am_K	0.2031(9)	am_D	0.748(7)
m_π/f_π	1.074(5)	m_K/f_K	3.206(20)	m_D/f_D	8.81(32)

References

[1] A. Abdel-Rehim et al. (ETM), Phys. Rev. **D95**, 094515 (2017), `1507.05068`

[2] Y. Iwasaki, Nucl. Phys. **B258**, 141 (1985)

[3] B. Sheikholeslami, R. Wohlert, Nucl. Phys. **B259**, 572 (1985)

[4] R. Frezzotti, G.C. Rossi, JHEP **08**, 007 (2004), `hep-lat/0306014`

[5] R. Frezzotti, G.C. Rossi, Nucl. Phys. Proc. Suppl. **128**, 193 (2004), [,193(2003)], `hep-lat/0311008`

[6] S.R. Sharpe, J.M.S. Wu, Phys. Rev. **D71**, 074501 (2005), `hep-lat/0411021`

[7] G. Herdoiza, K. Jansen, C. Michael, K. Ottnad, C. Urbach, JHEP **05**, 038 (2013), `1303.3516`

[8] S. Borsanyi et al., JHEP **09**, 010 (2012), `1203.4469`

[9] S. Aoki, R. Frezzotti, P. Weisz, Nucl. Phys. **B540**, 501 (1999), `hep-lat/9808007`

[10] P. Boucaud et al. (ETM), Comput. Phys. Commun. **179**, 695 (2008), `0803.0224`

[11] B. Kostrzewa, Ph.D. thesis, Humboldt-Universität zu Berlin, Mathematisch-Naturwissenschaftliche Fakultät (2017)

[12] S. Duane, A.D. Kennedy, B.J. Pendleton, D. Roweth, Phys. Lett. **B195**, 216 (1987)

[13] M. Hasenbusch, K. Jansen, Nucl. Phys. **B659**, 299 (2003), `hep-lat/0211042`

[14] M.A. Clark, A.D. Kennedy, Phys. Rev. Lett. **98**, 051601 (2007), `hep-lat/0608015`

[15] K. Jansen, C. Urbach, Comput. Phys. Commun. **180**, 2717 (2009), `0905.3331`

[16] S. Bacchio, C. Alexandrou, J. Finkenrath, A. Frommer, K. Kahl, M. Rottmann, PoS **LATTICE2016**, 259 (2016), `1611.01034`

[17] A. Frommer, K. Kahl, S. Krieg, B. Leder, M. Rottmann, SIAM J. Sci. Comput. **36**, A1581 (2014), `1303.1377`

[18] C. Alexandrou, S. Bacchio, J. Finkenrath, A. Frommer, K. Kahl, M. Rottmann, Phys. Rev. **D94**, 114509 (2016), `1610.02370`

[19] S. Bacchio, et al., **LATTICE2017** (2017)

[20] C. Alexandrou et al., in preparation (2017)

[21] J. Gasser, M.E. Sainio, A. Svarc, Nucl. Phys. **B307**, 779 (1988)

[22] B.C. Tiburzi, A. Walker-Loud, Phys. Lett. **B669**, 246 (2008), `0808.0482`

[23] C. Alexandrou, C. Kallidonis, Phys. Rev. **D96**, 034511 (2017), `1704.02647`

[24] M. Bruno, R. Sommer (ALPHA), PoS **LATTICE2013**, 321 (2014), `1311.5585`